HHS Public Access

Author manuscript

Immunohorizons. Author manuscript; available in PMC 2022 June 03.

Published in final edited form as:

Immunohorizons. ; 6(2): 144–155. doi:10.4049/immunohorizons.2200005.

Inactivation of SARS-CoV-2 and COVID-19 Patient Samples for Contemporary Immunology and Metabolomics Studies

Devon J. Eddins[*,†,‡], **Leda C. Bassit**[§,1], **Joshua D. Chandler**[†,¶,‖,1], **Natalie S. Haddad**[*,#], **Kathryn L. Musall**[§], **Junkai Yang**[*], **Astrid Kosters**[*], **Brian S. Dobosh**[†,¶,‖], **Mindy R. Hernández**[#], **Richard P. Ramonell**[#,2], **Rabindra M. Tirouvanziam**[†,¶,‖], **F. Eun-Hyung Lee**[*,‡,#], **Keivan Zandi**[§], **Raymond F. Schinazi**[§], **Eliver E. B. Ghosn**[*,†,‡]

[*]Lowance Center for Human Immunology, Division of Immunology and Rheumatology, Department of Medicine, Emory University School of Medicine, Atlanta, GA;

[†]Department of Pediatrics, Emory University School of Medicine, Atlanta, GA;

[‡]Emory Vaccine Center, Yerkes National Primate Research Center, Emory University School of Medicine, Atlanta, GA;

[§]Center for AIDS Research, Laboratory of Biochemical Pharmacology, Department of Pediatrics, Emory University School of Medicine and Children's Healthcare of Atlanta, Atlanta, GA;

[¶]Center for Cystic Fibrosis and Airways Disease Research, Children's Healthcare of Atlanta, Atlanta, GA;

[‖]Department of Pediatrics, Emory University School of Medicine, Atlanta, GA;

[#]Department of Medicine, Division of Pulmonary, Allergy, Critical Care and Sleep Medicine, Emory University School of Medicine, Atlanta, GA

Abstract

Due to the severity of COVID-19 disease, the U.S. Centers for Disease Control and Prevention and World Health Organization recommend that manipulation of active viral cultures of SARS-CoV-2 and respiratory secretions from COVID-19 patients be performed in biosafety level (BSL)3 laboratories. Therefore, it is imperative to develop viral inactivation procedures that permit samples to be transferred to lower containment levels (BSL2), while maintaining the fidelity of complex downstream assays to expedite the development of medical countermeasures. In this study, we demonstrate optimal conditions for complete viral inactivation following fixation of infected cells with commonly used reagents for flow cytometry, UVC inactivation in sera

Address correspondence and reprint requests to: Dr. Eliver E.B. Ghosn, Lowance Center for Human Immunology, Health Sciences Research Building, 1760 Haygood Drive NE, E240, Atlanta, GA 30322. eliver.ghosn@emory.edu.

[1]L.C.B. and J.D.C. contributed equally to this work.

[2]Current address: Division of Pulmonary, Department of Medicine, Allergy and Critical Care Medicine, University of Pittsburgh School of Medicine, Pittsburgh, PA.

The online version of this article contains supplemental material.

DISCLOSURES

F.E.-H.L. is the founder of MicroBplex, Inc., serves on the scientific advisory board of Be Biopharma, receives grants from the Bill & Melinda Gates Foundation and Genentech, and receives royalties from Berkeley Lights, Inc. The other authors have no financial conflicts of interest.

and respiratory secretions for protein and Ab detection, heat inactivation following cDNA amplification for droplet-based single-cell mRNA sequencing, and extraction with an organic solvent for metabolomic studies. Thus, we provide a suite of viral inactivation protocols for downstream contemporary assays that facilitate sample transfer to BSL2, providing a conceptual framework for rapid initiation of high-fidelity research as the COVID-19 pandemic continues.

INTRODUCTION

At the end of 2019, a novel betacoronavirus, SARS-CoV-2 (1), emerged from Wuhan in the Hubei Province of China, causing viral pneumonia that progressed to severe or critical disease in ~20% of infected patients, where in the most critical cases, patients would present with respiratory failure and require mechanical ventilator support in the intensive care unit (2–4). Since then, much research effort has been focused on better understanding pathogenesis and immunity to SARS-CoV-2 (5). However, due to the severity of disease, work with infectious patient samples (primarily samples from the airways) and active viral cultures require biosafety level (BSL)3 containment facilities as with other closely related betacoronaviruses, including SARS-CoV and Middle Eastern respiratory syndrome (MERS)–CoV (1, 6, 7). This can restrict research activity where containment facilities are not available. As the COVID-19 pandemic continues to surge with emergence of new variants (8), there is a continued need to conduct frontier research on COVID-19 immunology and pathogenesis to develop and refine medical countermeasures to protect at-risk populations and those disproportionately affected by COVID-19 disease (Refs. 9, 10, and D.J. Eddins, J. Yang, A. Kosters, V. Giacalone,X. Pechuan, J.D. Chandler, J. Eum, B.R. Babcock, B.S. Dobosh, M.R. Hernández, et al., manuscript posted on bioRxiv, DOI:10.1101/2021.06.02.446468). To facilitate this work, it is imperative to understand effective viral inactivation protocols that have minimal effects on assay readouts.

Although SARS-CoV-2 shares ~80% sequence homology with SARS-CoV (1), it is essential to evaluate the efficacy of existing inactivation procedures on novel, independent viral strains. For example, MERS-CoV is also closely related to SARS-CoV, but there are notable differences in the inactivation efficacy using gamma irradiation between the viruses (11, 12). Indeed, there have been earlier reports of efficient viral propagation and inactivation procedures for SARS-CoV-2 using heat, fixatives/chemicals/surfactants (e.g., formaldehyde/TRIzol/Triton X-100), and UVC irradiation (13–18), which are comparable to SARS-CoV and MERS-CoV (11, 12, 19–21). However, although most of these studies highlight efficient and effective viral inactivation protocols (14–18), the effects of inactivation on the fidelity of downstream assay readouts and analysis remain largely unknown. Specifically, a detailed report on viral inactivation protocols and how they influence contemporary immunology assays is notably lacking. Contemporary immunological assays including ELISA/Luminex/mesoscale assays for protein/Ab detection (D.J. Eddins et al., manuscript posted on bioRxiv, DOI:10.1101/2021.06.02.446468 and Refs. 22–24), metabolomics (25,26), high-dimensional flow cytometry (D.J. Eddins et al., manuscript posted on bioRxiv, DOI: 10.1101/2021.06.02.446468 and Refs. 27 and 28), and multiomics single-cell mRNA sequencing (scRNA-seq) (D.J. Eddins et al., manuscript posted on bioRxiv, DOI:

10.1101/2021.06.02.446468 and Refs. 29 and 30) are vital resources to develop and evaluate medical countermeasures for the ongoing COVID-19 pandemic.

To address the need to successfully inactivate virus and permit transfer of material from BSL3 to a lower containment (i.e., BSL2) environment for high-fidelity downstream assays, we examined the efficiency of several viral inactivation methods for contemporary immunological assays including flow cytometry, serology/protein detection, scRNA-seq, and high-throughput metabolomic experiments using both culture-derived virus and infected respiratory samples from COVID-19 patients. In this study, we report complete viral inactivation following fixation with 4% paraformaldehyde (PFA) or 1.6× BD FACS lysis solution (~2.5% formaldehyde and ~8.3% diethylene glycol) for 30 min at room temperature (RT) for flow cytometry, UVC inactivation at ~4000 μW/cm^2 for 30 min in sera and respire tory secretions for protein/Ab detection assays, heat inactivation following first-round cDNA amplification of single-cell emulsions for droplet-based scRNA-seq, and metabolite extraction for 30 min with 2 and 4 vol (66% and 80% final volume) of a 1:1 acetonitrile/methanol solution with 12.5 μM benzoyl-D5-hippuric acid at 4°C for metabolomic studies. These results will serve as conceptual framework and promote rapid initiation of cutting-edge immunology studies as the COVID-19 pandemic continues to evolve and for other risk group three agents that require higher containment.

MATERIALS AND METHODS

Ethics and biosafety statements

COVID-19$^+$ patients were recruited from the Intensive Care Units of Emory University, Emory St. Joseph's, Emory Decatur, and Emory Midtown Hospitals (severe) or the Emory Acute Respiratory Clinic (mild), and healthy adults were recruited from the Emory University Hospital. All studies were approved by the Emory Institutional Review Board under protocol numbers IRB00058507, IRB00057983, and IRB00058271. Informed consent was obtained from the patients when they had decision-making ability or from a legal authorized representative when the patient was unable to provide consent. We collected both blood and non-induced sputum (healthy/mild) or endotracheal aspirate (ETA; severe). Study inclusion criteria included a confirmed COVID-19 diagnosis by PCR amplification of SARS-CoV-2 viral RNA (vRNA) obtained from nasopharyngeal/oropharyngeal swabs, age of ≥18 y or greater, and willingness and ability to provide informed consent. All work with infectious virus and respiratory samples from COVID-19 patients was conducted inside a biosafety cabinet within the Emory Health and Safety Office– and U.S. Department of Agriculture–approved BSL3 containment facility in the Health Sciences Research Building at Emory University following protocols approved by the Institutional Biosafety Committee and Biosafety Officer.

Virus and cells

African green monkey (*Cercopithecus aethiops*) kidney epithelial cells (Vero E6 cells; ATCC CRL-1586) were maintained in complete DMEM containing 1× DMEM supplemented with 25 mM HEPES, 2 mM L-glutamine,1 mM sodium pyruvate, 1× non-essential amino acids, 1× antibiotic/antimycotic solution (all from Corning Life Sciences) and

10% heat-inactivated FBS (Life Technologies), unless indicated otherwise. Human lung adenocarcinoma epithelial cells (Calu-3 cells; ATCC HTB-55) were maintained in complete MEM (cMEM) containing 1× MEM (Corning Life Sciences) supplemented with 1× antibiotic/antimycotic solution and 10% heat-inactivated FBS unless indicated otherwise. Primary leukocytes from the airways of severe COVID-19 patients were collected bedside via endotracheal aspiration, and whole blood was collected by standard venipuncture, then processed as previously described (D.J. Eddins et al., manuscript posted on bioRxiv, DOI: 10.1101/2021.06.02.446468). SARS-CoV-2 USA-WA1/2020 (hereafter SCV2-WA1) was provided by BEI Resources (Manassas, VA, USA). Virus was propagated in Vero E6 cells as previously described (15, 31), and titer was determined by 50% tissue culture infective dose ($TCID_{50}$/ml) or plaque assays (PFU/ml). Low-passage (P1 or P2) virus stocks were used throughout this study.

Infectivity assays

Plaque assays with methylcellulose.—Vero E6 cells were seeded in six-well plates (BD Falcon) with 5×10^5 cells/well in 5% DMEM 24 h prior to infection and checked to verify ≥80% confluency. Ten-fold dilutions of virus, respiratory secretions, and/or scRNA-seq emulsion in serum-free DMEM (200 μL)were incubated on Vero E6 monolayers for 1 h absorption at 37°C with rocking at 15-min intervals. After absorption, cells were overlaid with 2% methylcellulose (MilliporeSigma) in 2% DMEM for 72 h at 37°C in a 5% CO_2, humidified incubator. At 72 h postinfection (hpi), methylcellulose was carefully removed and cells were gently rinsed once with 1× HBSS (Corning Life Sciences). Monolayers were fixed and plaques visualized with a solution of 0.4% crystal violet by weight in 80% methanol (MilliporeSigma) and 4% PFA (Electron Microscopy Sciences) for 20 min at RT.

Plaque assays with agarose.—Vero E6 cells were seeded in six-well plates with 5×10^5 cells/well in 5% DMEM 24 h prior to infection and checked to verify ≥80% confluency. Ten-fold dilutions of virus, respiratory secretions, and/or scRNA-seq emulsion in serum-free DMEM (200 μl) were incubated on Vero E6 monolayers for 1 h absorption at 37°C with rocking at 15-min intervals. After absorption, cells were overlaid with 2 ml of 0.5% immunodiffuse agarose (MP Biomedicals) in 1× DMEM supplemented with 5% FBS, 2 mM L-glutamine, 1 mM sodium pyruvate, 1× non-essential amino acids, 1× sodium bicarbonate, and 1× antibiotic/antimycotic solution. At 72 hpi, a second 2-ml overlay of 0.5% immunodiffuse agarose in a 1× HBSS solution with 0.026% neutral red (MilliporeSigma) was added for ≥3 h to visualize plaques.

$TCID_{50}$ assays.—Vero E6 cells were seeded in 96-well plates with 2×10^4 cells/well in 5% MEM 24 h prior to infection and checked to verify ≥80% confluency. Ten-fold dilutions of stock SCV2-WA1 virus in serum-free MEM (100 μl) were incubated on Vero E6 monolayers in quadruplicates for 2-h absorption at 37°C without rocking. Following absorption, the inoculum was removed and cells were cultured in 2% MEM. Cells were assessed daily for cytopathic effect compared with mock-infected negative controls by microscopy for 6 d. Calculations for $TCID_{50}$ were performed using either the Spearman–Käber (32) or Reed and Muench (33) methods as previously described (34).

Focus reduction neutralization assays.—Vero E6 cells were seeded in 96-well plates with 2×10^4 cells/well in 5% DMEM 24 h prior to infection and checked to verify ≥80% confluency. Dilutions of virus and/or virus treated with inactivation reagents in Opti-MEM (50 μl) were incubated on Vero E6 monolayers for 2 h absorption at 37°C without rocking. After absorption, cells were overlaid with 2% methylcellulose in Opti-MEM (Life Technologies) supplemented with 2% FBS, 2.5 μg of amphotericin B (MilliporeSigma), and 20 μg/ml ciprofloxacin (MilliporeSigma) for 72 h at 37°C in a 5% CO_2, humidified incubator. At 72 hpi, methylcellulose was carefully removed and the cells were fixed with a 1:1 methanol/acetone mixture for 30 min at RT, then blocked with 200 μl of 5% milk in 1× PBS for 20 min.Cells were incubated with an anti–SARS-CoV-2 spike receptor-binding domain polyclonal Ab (Gentaur) at 1:3000 overnight at 37°C. Cells were washed to remove excess Ab, then incubated with a secondary HRP-conjugated anti-human IgG for 1 h at 37°C. Cells were washed to remove excess Ab and foci were visualized using the TrueBlue peroxidase substrate (SeraCare Life Sciences) incubated for 1 h at RT with rocking prior to imaging with an ELISPOT reader for foci quantification. Data are reported as focus forming units per milliliter.

Inactivation by fixative solutions

Vero E6 cells were infected at a multiplicity of infection (MOI) of 0.01 and cultured in six-well plates for 48 h with cMEM or cells from ETAs of COVID-19–infected patients were fixed with a freshly prepared 2% or 4% PFA solution (20% stock diluted in 1× HBSS; Electron Microscopy Sciences) or a 1.6× BD FACS lysis solution (1:6 in sterile dH_2O; BD Biosciences) for the indicated time points at RT. Unfixed cells were incubated with 1× HBSS. Following fixation, cells from each condition were washed twice and resuspended in cMEM for an additional 48 h incubation at 37°C in a humidified, 5% CO_2 incubator. Culture supernatants were then collected and either plated immediately or frozen at −80°C for analysis by plaque assay.

Inactivation by UVC radiation

Fifty- to 1000-μl aliquots of SCV2-WA1 virus stock (2.1×10^5 PFU/ml), respiratory supernatant (additional samples combined with our previous data [D.J. Eddins et al., manuscript posted on bioRxiv, DOI: 10.1101/2021.06.02.446468]), or patient sera were collected for UV inactivation. Samples were positioned 2–3 cm from the light source and exposed to 254 nm of UVC light at maximum intensity (~4000 μW/cm^2) for 30 min using a Spectrolinker XL-1000 UV crosslinker (Spectronics) in either clear 2-ml microcentrifuge tubes (positioned on their side) or a 96-well plate (with the lid removed). Samples were either plated immediately or frozen at −80°C for analysis by plaque assay.

Inactivation for metabolomic assays

To assess a nontoxic concentration of the metabolite extraction solvent (50% acetonitrile, 50% methanol, and 12.5 μM/l D5-benzoylhippuric acid) for subsequent focus reduction neutralization assays (FRNAs), cytotoxicity tests were performed in Vero E6 cells via an MTS (3-(4,5-dimethylthiazol-2-yl)-5-(3-carboxymethoxyphenyl)-2-(4-sulfophenyl)-2H-tetrazolium, inner salt) assay using the CellTiter 96 non-radioactive cell proliferation kit

(Promega) as previously described (35). Uninfected Vero E6 cells were incubated with the extraction solvent, diluted in Opti-MEM at 1:10, 1:100, and 1:1000 in triplicate at 37°C, 5% CO_2 for 72 h with 100, 10, and 1 μM cycloheximide as a positive control. After 72 h, the MTS compound was added to the cells and incubated for an additional 2 h. To determine the number of viable cells in each well, the absorbance was measured at 490 nm using a 96-well plate reader (BioTek). Cytotoxicity was expressed as the dilution of the extraction solvent that inhibited cell proliferation by 50% (IC_{50}) and calculated using the Chou and Talalay method (36). SCV2-WA1 (2.5×10^4 $TCID_{50}$/ml) was incubated with or without the extraction solvent (1:2 or 1:4) or Triton X-100 for 30 min at 4°C, then centrifuged at 20,000 × *g* for 10 min at 4°C. Supernatants were collected and diluted in Opti-MEM to final concentrations of 1:100 for the extraction solvent or 1% Triton X-100, and >100 focus-forming units/ml SARS-CoV-2 per well for analysis by FRNAs.

Inactivation for scRNA-seq (10x Genomics)

SARS-CoV-2–infected Vero E6 cells (MOI of 0.04 for 72 h) or Calu-3 cells (MOI of 0.04 for 48 h) were encapsulated for scRNA-seq following the manufacturer's protocol ("Chromium next GEM single cell V(D)J reagent kits v1.1 user guide with feature barcode technology for cell surface protein"; document number CG000208; 10x Genomics) targeting 20,000 and 10,000 cells, respectively. An aliquot of the emulsion was collected following encapsulation for analysis by a plaque assay. The remaining emulsion was processed for cDNA synthesis reaction following the manufacturer's protocol with reagent volumes adjusted to reflect the reduced reaction volume after taking aliquots for plaque assays. The PCR amplification profile was 45 min at 53°C followed by 5 min at 85°C. An additional aliquot of the cDNA suspension was collected following PCR reactions and either plated immediately or frozen at −80°C for analysis by plaque assay. Plaque assays were also performed on the encapsulation emulsion alone (without including virus-infected cells) to evaluate reagent cytotoxicity on Vero E6 monolayers.

Luminex proteomic serology assays

Plasma from whole blood of COVID-19 patients was isolated via centrifugation at 400 × *g* for 10 min at 4°C. To remove platelets, the isolated plasma was centrifuged at 4000 × *g* for 10 min at 4°C. Plasma samples were stored at −80°C until analyzed. Luminex serology assays were performed as previously described (23). In brief, ~50 μl of coupled microsphere mix was added to each well of 96-well clear-bottom black polystyrene microplates (Greiner Bio-One) at a concentration of 1000 microspheres per region per well. All wash steps and dilutions were performed with 1% BSA in 1× PBS (hereafter assay buffer). Sera were assayed at 1:500 dilutions (in assay buffer) and surveyed for anti–SARS-CoV-2 nucleocapsid or receptor-binding domain Abs by 1-h incubation on a plate shaker at 800 rpm in the dark. Following incubation, wells were washed five times with 100 μl of assay buffer using a BioTek 405 TS plate washer, then 3 mg/ml PE-conjugated goat anti-human IgA, IgG, and/or IgM (SouthernBiotech) was applied. After a 30-min incubation, wells were washed three times in 100 μl of assay buffer, then resuspended in 100 μl of assay buffer for acquisition and analysis using a Luminex FLEXMAP 3D instrument and xPONENT 4.3 software (Luminex). Mean fluorescence intensity (MFI) using combined or individual detection Abs (i.e., anti-IgA, anti-IgG, or anti-IgM) was

measured and the background value of assay buffer was subtracted from each serum sample result to obtain MFI minus background values (net MFI). Data were imported to Prism 9 for graphing and statistical analyses. Data were analyzed for distribution (normal [Gaussian] versus lognormal) independently using the D'Agostino and Pearson test for normality in the untransformed and $\log_{10}$-transformed data. In cases where the total sample size (N) was too small for the D'Agostino and Pearson normality test, the Shapiro–Wilk test was used to assess distribution. When data passed both distribution tests, the likelihood of each distribution (normal versus lognormal) was computed, and quantile–quantile (QQ) plots were generated. When untransformed and $\log_{10}$-transformed data had a higher likelihood of a normal distribution (passing normal distribution test) and/or failed lognormal distribution test, two-tailed paired ratio *t* tests were performed to compare untreated and UVC-treated samples. In all instances where the lognormal distribution was likely non-parametric, Wilcoxon matched-pairs signed rank tests were performed.

Metabolomic assays

Metabolites in human plasma were extracted from the National Institute of Standards and Technology (NIST) "Standard Reference Materials 1950" after mock or UVC treatment by addition of 4 vol of 50% acetonitrile, 50% methanol, and 12.5 μM/l benzoyl-D5-hippuric acid (extraction solvent). Samples were vortexed for 10 s, incubated on ice for 30 min, and then centrifuged at 20,000 × *g* for 10 min at 4°C. The clear supernatant was aliquoted and injected (2.5 μl) on a Vanquish Horizon liquid chromatograph coupled to Q Exactive high-field mass spectrometer (Thermo Fisher Scientific). A 150- × 2.1-mm ZIC-HILIC (MilliporeSigma) column and matching guard column were used to separate polar metabolites. Metabolites were ionized in both positive and negative mode and analyzed in full scan mode (67–1000 *m/z*). Pooled quality control samples comprising equal proportions of every study sample were used to generate ddMS2 (Top20N) spectra of metabolites, evaluate assay reproducibility, and correct batch drift. Compound Discoverer 3.2 (Thermo Fisher Scientific) was used to quantify peak areas and assign annotations based on a local library of reference standards or via matching metabolites to reference spectra in mzCloud (mzcloud.org). Data were imported to Prism 9 for graphing and statistical analyses by unpaired *t* tests for untreated versus UVC-treated replicates, assuming individual variance, using the adaptive linear (two-step) step-up (Benja-mini, Krieger, and Yekutieli) method (37) to control the false discovery rate (FDR), and a desired FDR (Q) of 10% for multiple comparisons.

scRNA-seq data alignment, dimensionality reduction, and clustering

The Cell Ranger software (v.5.0.0; 10x Genomics) was used to perform cell barcode processing and single-cell 5′ unique molecular identifier (UMI) counting. To detect SARS-CoV-2 reads, a customized reference genome was built by integrating human GRCh38 and SARS-CoV-2 genomes (SARS-CoV-2 isolate Wuhan-Hu-1, complete genome, GenBank MN908947.3). Splicing-aware aligner STAR (38) was used in FASTQ alignments. Cell barcodes were then determined based on the distribution of UMI counts automatically. The filtered gene–barcode matrices were first normalized using the "LogNormalize" method in Seurat v.3 (39) with default parameters. The top 2000 variable genes were then identified using the "vst" method by the "FindVariableFeatures" function. Principal component

analysis (PCA) was performed using the top 2000 variable genes, and then uniform manifold approximations and projections were generated using the top 30 principal components to visualize cells. Graph-based clustering was performed on the principal component analysis–reduced data for clustering analysis with the resolution set to 0.8 to obtain the clusters. The total viral UMIs were the sum of the UMIs of the 12 SARS-CoV-2 genes (40).

SARS-CoV-2 quantitative reverse transcription PCR

Stock SCV2-WA1 virus and patient samples (400 μl) were thoroughly mixed 1:1 with 2× DNA/RNA Shield and incubated at RT for 20 min for inactivation, and vRNA was extracted using the Quick-RNA viral kit (Zymo Research) following the manufacturer's protocol. cDNA was synthesized using a high-capacity cDNA reverse transcription kit (Applied Biosystems) per the manufacturer's instructions and diluted 1:5 in nuclease-free water, and then 10 ml of diluted cDNA was used with the NEB Luna universal probe qPCR mastermix (New England BioLabs) following the manufacturer's protocol, and quantitative reverse transcription PCR (RT-qPCR) was performed in 384-well plates using a QuantStudio 5 real-time PCR system (Applied Biosystems). Primer/probe pairs were 5'-AGAAGATTGGTTAGATGATGATAGT-3' (forward primer), 5'-TTCCATCTCTAATTGAGGTTGAACC-3' (reverse primer), and 5'-/5(6)-FAM/TCCTCACTGCCGTCTTGTTGACCA/3IABk-FQ/−3 (probe), which were designed from sequences previously described (41) (Integrated DNA Technologies). To generate a standard curve and quantify SARS-CoV-2 genome copies, a gBlock with the sequence 5'-AATTAAGAACACGTCACCGCAAGAAGAAGATTGGTTAGATGATGATAGTCAACAAACTGTTGGTCAACAAGACGGCAGTGAGGACAATCAGACAACTACTATTCAAACAATTGTTGAGGTTCAACCTCAATTAGAGATGGAACTTACAGTTTCAGTGTTCAATTAA-3' (Integrated DNA Technologies) was used as a standard.

To determine PFU equivalent (ePFU) values from respiratory samples, vRNA was extracted from 10-fold serial dilutions of stock SCV2-WA1 of a known titer for RT-qPCR to generate a standard curve from which the number of genome copies per PFU could be extrapolated as previously described (42). Culture supernatants from mock- (1× HBSS) and SARS-CoV-2–infected Calu-3 (MOI 0.04) cells were used as additional controls.

RESULTS

Inactivation by fixation

To evaluate the ability of commonly used fixatives in flow cytometry (here, formaldehyde-based and PFA) to completely inactivate SARS-CoV-2–infected cells for transfer to lower containment settings, we performed a time course of inactivation (Fig. 1A) using 2% and 4% PFA (diluted from a 20% stock, see Materials and Methods) along with 1.6× BD FACS lysis solution (10× stock diluted 1:6 in sterile dH_2O). Cells exposed to 2% and 4% PFA for 15 min at RT were still able to produce infectious virus when returned to culture for 48 h (Fig. 1B, 1C), with a decrease in viral titer (PFU/ml). This is in contrast to a previous report that indicated a 10-min treatment with 4% PFA is sufficient to inactivate virus (13). However, infectious virus was not detected by a plaque assay following 15 min of exposure to 1.6× BD FACS lysis solution and at all subsequent time points (Fig. 1B, 1C). Cells treated

with 4% PFA for 30 min at RT were no longer infectious; however, 60 min was required to fully inactivate virus in cells treated with 2% PFA at RT. These data indicate that common fixation protocols (30 min fixation at RT) for commercially available fixatives, specifically those with ≥4% PFA, are sufficient for inactivating SARS-CoV-2–infected cells.

UVC inactivation

Inactivation of respiratory secretions and viral stocks.—Although complete inactivation of SARS-CoV viral stocks can be achieved with <15 min of exposure to UVC irradiation (11), a follow-up report for SARS-CoV inactivation in non-cellular blood products in PBS solutions recommended 40 min of exposure to inactivate virus (19). Therefore, we selected 30 min of exposure to UVC irradiation at maximum intensity (~4000 $\mu W/cm^2$) for both culture-derived SARS-CoV-2 viral stocks and respiratory secretions from COVID-19 patients. First, we determined viral load in the respiratory secretions by extrapolating ePFU/ml from RT-qPCR results of respiratory secretions (*see* Materials and Methods) (42). Using a standard curve generated from virus stock of a known titer (Fig. 2A), we determined 1 PFU to be equivalent to 73 SARS-CoV-2 genome copies in RT-qPCR data. This allowed for more accurate viral detection and quantification (Fig. 2B) since ETA and bronchoalveolar lavage fluid samples are standard modalities used to diagnose ventilator-associated pneumonia (43, 44) and can be inundated with pulmonary microbes that grow in cultures, confounding traditional plaque assays (see Supplemental Fig. 1). As expected from our previous study, we found that viral load varied across patient groups where those with severe disease had lower (or absent) viral load at the time of sampling (samples were combined with our previous data in D.J. Eddins, et al., manuscript posted on bioRxiv, DOI: 10.1101/2021.06.02.446468; Fig. 2B). Following 30 min of exposure to UVC irradiation, both virus stock (2.1×10^5 PFU/ml) and respiratory secretions were not detected by plaque assay (Fig. 3C), indicating complete viral inactivation. Additionally, we demonstrate that UVC inactivation abolishes microbial growth in plaque assays that hampered accurate viral load detection in ETA samples (Supplemental Fig. 1), which is consistent with the established efficacy of UVC inactivation for a diverse range of pathogenic microbes (45, 46).

Effects on Ab measurements.—To determine the effect of 30 min of exposure to UVC irradiation on protein/Ab detection, we compared untreated and UVC-treated plasma samples from both mild and severe COVID-19 patients (Fig. 2D). We did not observe any substantial differences in the levels of anti–SARS-CoV-2 Abs detected by Luminex proteomic assays. In patients with mild COVID-19 symptoms, Ab measurements against the Spike protein subunit 1 (S1) and the N-terminal domain (NTD) achieved statistical significance; however, differences between untreated and UVC-treated samples were consistently ≤10% for all individual replicates (average difference between pairs is 5.47% and 7.79% for the S1 and the NTD, respectively). All other targets for mild samples and all targets for severe samples were not significantly different. Collectively, these data indicate that 30 min of exposure to UVC irradiation at maximum intensity (~4000 $\mu W/cm^2$) is both effective for inactivating high-titer stock SARS-CoV-2 and respiratory secretions from COVID-19 patients, with minimal effect on downstream protein/Ab assays.

Inactivation for metabolomics

UVC treatment.—To determine an optimal inactivation procedure for metabolomics, we first evaluated the effects of UVC inactivation described above on Standard Reference Material 1950 of metabolites in human plasma (47). UVC inactivation significantly altered the metabolic profile of samples (Fig. 3A). We show that the differentially expressed metabolites between untreated and UVC-treated plasma samples are redox-active metabolites (Fig. 3B), suggesting that reactive oxygen species known to be produced during UVC irradiation (48) lead to sample oxidation during this procedure, similar to reactive oxygen species oxidation in vivo (49–51). Therefore, UVC inactivation is not suitable for metabolomic studies, especially when interrogating redox-active metabolites.

Treatment with organic solvents.—We then wanted to test whether a standard metabolomic sample extraction procedure with organic solvents (*see* Materials and Methods) could successfully inactivate SARS-CoV-2–infected non-cellular products (such as respiratory secretions or plasma) as an alternative to UVC inactivation. Specifically, we used a 1:1 mixture of acetonitrile and methanol including a deuterated internal standard, administered at 4 vol relative to the starting sample. We performed FRNAs with stock SCV2-WA1 (untreated) and virus treated with either the extraction solvent or Triton X-100, which has been shown to inactivate SARS-CoV-2 (16, 17). Incubation of SCV2-WA1 virus stock 1:4 with the extraction solvent was sufficient to fully inactivate virus along with Triton X-100 (Fig. 3C). Cells incubated with the extraction solvent remained viable (Fig. 3C), confirming virus inactivation independent of Vero E6 cytotoxicity, which was observed for other chemical reagents/surfactants such as Triton X-100 (Fig. 3C). We additionally tested incubation of SCV2-WA1 virus stock 1:2 with the extraction solvent, which was also sufficient to fully inactivate virus (Supplemental Fig. 2), providing the flexibility of using a relatively less concentrated organic extraction solution and could improve assay sensitivity. Therefore, these results demonstrate that a standard metabolomic assay sample processing procedure with either 2 or 4 vol of our extraction solvent is sufficient to inactivate SARS-CoV-2–infected non-cellular samples while retaining sample integrity as compared with UVC inactivation.

Inactivation for scRNA-seq

To better understand efficacy of SARS-CoV-2 inactivation in droplet-based scRNA-seq pipelines–specifically the 10x Genomics platform–we evaluated viral inactivation at the two early steps in the manufacturer's instructions. First, we evaluated the reagent cytotoxicity of the 10x Genomics encapsulation emulsion on Vero E6 cells by performing plaque assays with the emulsion free of encapsulated cells. We demonstrate that the reagents in the emulsion (many of which are proprietary) are not inherently cytotoxic to Vero E6 monolayers, allowing us to evaluate viral inactivation by a standard plaque assay (Fig. 4A).

We next evaluated the efficacy of viral inactivation following single-cell encapsulation (which contains a proprietary lysis solution) of SCV2-WA1–infected (MOI of 0.04) Vero E6 or Calu-3 cells. We show that the standard single-cell encapsulation step alone is not sufficient to fully inactivate SARS-CoV-2, which could be detected in subsequent plaque assays (Fig. 4A, 4B). Therefore, we tested the efficacy of the cDNA synthesis reaction,

which includes exposure to temperatures ≥53°C, in viral inactivation. We show that after the PCR reaction (45 min at 53°C followed by 5 min at 85°C), infectious SARS-CoV-2 was not detectable by plaque assay (Fig. 4A, 4B). Taken together, our data demonstrate that scRNA-seq emulsions of SARS-CoV-2–infected cells are fully inactivated only after heat inactivation following the cDNA synthesis reaction using the conditions described in the manufacturer's protocol (45 min at 53°C followed by 5 min at 85°C), which can then be transferred to lower containment for library preparation and sequencing. Indeed, after sequencing, we found >2.3 million viral transcripts (UMIs) in ~8000 SCV2-WA1–infected Calu-3 cells (Fig. 4C).

DISCUSSION

To date, there have been multiple studies to evaluate efficacy of viral inactivation procedures using heat, chemicals, and UVC irradiation on SARS-CoV-2–infected samples (13–17). Many of these studies have evaluated traditional procedures established for SARS-CoV and MERS-CoV and were found to have comparable efficacies (11, 12, 19, 20). In the present study, we add to these studies by evaluating inactivation procedures performed under optimized conditions that allow for downstream processing/analysis for contemporary immunology assays with limited effects on assay readouts. We caution that all procedures are performed under the specified conditions, and those that differ from what have been described in the present study should be evaluated on viral stocks and patient samples before transferring to lower biosafety containment.

Since its induction in the 1960s, flow cytometry has been the preeminent technology for single-cell analysis (52, 53), particularly for investigating the heterogeneity of the immune system in health and disease (54, 55). Indeed, high-dimensional flow cytometry has been a pivotal tool in dissecting the complex immunophenotypes of leukocytes in COVID-19 (D.J. Eddins et al., manuscript posted on bioRxiv, DOI: 10.1101/2021.06.02.446468 and Refs. 27, 28, 56, 57). We evaluated the ability of commercially available fixatives commonly used in flow cytometry (formaldehyde-based) to fully inactivate SARS-CoV-2–infected cells to facilitate transfer of cells from BSL3 to BSL2 for data acquisition (D.J. Eddins et al., manuscript posted on bioRxiv, DOI: 10.1101/2021.06.02.446468). In this study, we show that treatment with 4% PFA or 1.6× BD FACS lysis solution for 30 min at RT was sufficient to completely inactivate SARS-CoV-2–infected cells, even at viral titers higher than in cells from infected patients. Therefore, most common fixation protocols and reagents (e.g., BD Cytofix/Cytoperm, BioLegend fixation buffer) that contain ≥4% PFA are suitable for preparing fluorescently stained, SARS-CoV-2–infected cells for transfer out of BSL3 containment after 30 min of exposure at RT. Conversely, lower concentrations of PFA (i.e., 2%) required longer exposure time (at least 60 min at RT) to fully inactivate samples.

Similarly, we show that UVC irradiation (~4000 μW/cm^2) for 30 min is sufficient to fully inactivate high-titer SCV2-WA1 viral stocks and respiratory supernatants from patients with minimal effects on protein/Ab detection (58), which will promote further studies on secretions from ETAs and/or bronchoalveolar lavage fluid to better understand local versus systemic responses (D.J. Eddins et al., manuscript posted on bioRxiv, DOI: 10.1101/2021.06.02.446468 and Ref. 24). Importantly, note that a previous study on

UVC inactivation of SARS-CoV found BSA to protect virus from UVC inactivation even after 60 min of exposure (19). Therefore, we avoided BSA in solutions used in respiratory sample preparation (D.J. Eddins et al., manuscript posted on bioRxiv, DOI: 10.1101/2021.06.02.446468), and plasma samples were inactivated prior to dilution in the Luminex proteomic assay buffer (1% BSA in 1× PBS, see Materials and Methods).

Despite having negligible effects in the proteomic assays, we did observe that UVC inactivation significantly altered metabolomic profiles is human plasma samples. Specifically, we show that redox-active metabolites such as methionine and urate are oxidized following UVC inactivation, significantly increasing signals for methionine sulfoxide and allantoin, respectively (49, 50). Similarly, bilirubin, which is oxidized to biliverdin (51), is significantly decreased with UVC treatment. Therefore, UVC inactivation of clinical samples could lead to misleading biological interpretations, artificially skewing sample metabolites to a more oxidized profile (49–51). However, high-concentration methanol (≥80%) (59, 60) and methanol/acetone mixtures (12, 21) have previously been shown to successfully inactivate many viral-infected samples, including SARS-CoV-2 (16–18). The extraction solvent we used is similar to that used in many metabolomic sample preparation techniques and was sufficient to inactivate virus while maintaining data integrity.

Systems immunology approaches, including multiomic scRNA-seq, have greatly advanced our understanding of COVID-19 immunity and pathogenesis (D.J. Eddins et al., manuscript posted on bioRxiv, DOI: 10.1101/2021.06.02.446468 and Refs. 29 and 30). However, a detailed report on inactivation efficacy of scRNA-seq pipelines is notably lacking. We demonstrate that in the standard 10x Genomics pipeline encapsulation alone was insufficient to fully inactivate virus. According to the manufacturer's guidelines, a cDNA synthesis reaction is the next immediate step after encapsulation (*see* Materials and Methods). Although many studies have evaluated the efficacy of heat inactivation for SARS-CoV-2 and demonstrated 45 min at 56°C and 5 min at 100°C are sufficient to fully inactivate virus (13–18), none has tested the specific conditions for the cDNA synthesis reaction (45 min at 53°C followed by 5 min at 85°C). In this study, we expand on the previous report by demonstrating that the cDNA synthesis reaction in the standard 10x Genomics pipeline successfully inactivates SARS-CoV-2 and allows for transfer to lower containment for subsequent processing and library generation procedures.

Thus, we report optimized methods of viral inactivation that have minimal, if any, adverse impact on immunological studies of infected culture-derived and patient samples, permitting safe transfer to lower containment laboratories (BSL2) for final processing and data acquisition. Taken together, this suite of inactivation procedures can serve as guidelines for rapid initiation of research as the COVID-19 pandemic continues.

Supplementary Material

Refer to Web version on PubMed Central for supplementary material.

ACKNOWLEDGMENTS

We thank Fred Souret (10x Genomics) for providing additional reaction kits to test viral inactivation in scRNA-seq assays, Doan Nguyen for technical direction with the serology experiments, and the Emory Pediatric/Winship Flow Cytometry Core (access supported in part by Children's Healthcare of Atlanta) for support with flow cytometry experiments. We thank Rafi Ahmed (Emory University School of Medicine) and Jacob Kohlmeier (Emory University School of Medicine) for providing the Vero E6 and Calu-3 cell lines, respectively. We thank Ann Chahroudi, Nils Schoof, Kira Moresco, and Stacy Heilman of the Department of Pediatrics (Emory University School of Medicine), along with the Emory Biosafety Officers Kalpana Rengarajan and Esmeralda Meyer and the Institutional Biosafety Committee (IBC), for assistance with the BSL3 facility and protocol review/approval.

This work was supported by National Institutes of Health (NIH) National Institute of Allergy and Infectious Diseases R01AI123126 and R01-AI123126-05S1 (awarded to E.E.B.G.), R01-AI161570 (awarded to R.F.S.), NIH National Heart, Lung, and Blood Institute T32-HL116271-07 (awarded to R.P.R.), the Program for Breakthrough Biomedical Research and Lowance Center for Human Immunology (awarded to E.E.B.G.), National Science Foundation Early-concept Grants for Exploratory Research Award 2032273 and the Woodruff Health Science Center COVID-19 CURE award (awarded to R.M.T., R.F.S., and K.Z.). D.J.E. was supported in part by the Laney Graduate School Fellowship (Emory University) and J.D.C. was supported in part by CF@LANTA, a component of Emory University and Children's Healthcare of Atlanta.

Abbreviations used in this article:

BSL	biosafety level
cMEM	complete MEM
ePFU	equivalent PFU
ETA	endotracheal aspirate
FDR	false discovery rate
FRNA	focus reduction neutralization assay
hpi	hour postinfection
MERS	Middle Eastern respiratory syndrome
MOI	multiplicity of infection
NIST	National Institute of Standards and Technology
NTD	N-terminal domain
PFA	paraformaldehyde
RT	room temperature
RT-qPCR	quantitative reverse transcription PCR
S1	Spike protein subunit 1
scRNA-seq	single-cell RNA sequencing
$TCID_{50}$	50% tissue culture infective dose
UMI	unique molecular identifier
vRNA	viral RNA

REFERENCES

1. Gorbalenya AE, Baker SC, Baric RS, de Groot RJ, Drosten C,Gulyaeva AA, Haagmans BL, Lauber C, Leontovich AM, Neuman BW, et al. ; Coronaviridae Study Group of the International Committee on Taxonomy of Viruses. 2020. The species severe acute respiratory syndrome-related coronavirus: classifying 2019-nCoV and naming it SARS-CoV-2. Nat. Microbiol 5: 536–544. [PubMed: 32123347]
2. Huang C, Wang Y, Li X, Ren L, Zhao J, Hu Y, Zhang L, Fan G,Xu J, Gu X, et al. 2020. Clinical features of patients infected with 2019 novel coronavirus in Wuhan, China. Lancet 395: 497–506. [PubMed: 31986264]
3. Merad M, and Martin JC. 2020. Pathological inflammation in patients with COVID-19: a key role for monocytes and macrophages. [Published erratum appears in 2020 Nat. Rev. Immunol. 20: 448.] Nat. Rev. Immunol 20: 355–362. [PubMed: 32376901]
4. Wu C, Chen X, Cai Y, Xia J, Zhou X, Xu S, Huang H, Zhang L, Zhou X, Du C, et al. 2020. Risk factors associated with acute respiratory distress syndrome and death in patients with coronavirus disease 2019 pneumonia in Wuhan, China. JAMA Intern. Med 180: 934–943. [PubMed: 32167524]
5. Carvalho T, Krammer F, and Iwasaki A. 2021. The first 12 months of COVID-19: a timeline of immunological insights. Nat. Rev. Immunol 21: 245–256. [PubMed: 33723416]
6. de Wit E, van Doremalen N, Falzarano D, and Munster VJ. 2016. SARS and MERS: recent insights into emerging coronaviruses. Nat. Rev. Microbiol 14: 523–534. [PubMed: 27344959]
7. Graham RL, Donaldson EF, and Baric RS. 2013. A decade after SARS: strategies for controlling emerging coronaviruses. Nat. Rev. Microbiol 11: 836–848. [PubMed: 24217413]
8. Harvey WT, Carabelli AM, Jackson B, Gupta RK, Thomson EC,Harrison EM, Ludden C, Reeve R, Rambaut A, Peacock SJ, and Robertson DL; COVID-19 Genomics UK (COG-UK) Consortium. 2021. SARS-CoV-2 variants, spike mutations and immune escape. Nat. Rev. Microbiol 19: 409–424. [PubMed: 34075212]
9. Romano SD, Blackstock AJ, Taylor EV, El Burai Felix S, Adjei S, Singleton CM, Fuld J, Bruce BB, and Boehmer TK. 2021. Trends in racial and ethnic disparities in COVID-19 hospitalizations, by region–United States, March–December 2020. MMWR Morb. Mortal. Wkly. Rep 70: 560–565. [PubMed: 33857068]
10. Van Dyke ME, Mendoza MCB, Li W, Parker EM, Belay B,Davis EM, Quint JJ, Penman-Aguilar A, and Clarke KEN. 2021. Racial and ethnic disparities in COVID-19 incidence by age, sex, and period among persons aged <25 years–16 U.S. Jurisdictions, January 1–December 31, 2020. MMWR Morb. Mortal. Wkly. Rep 70: 382–388. [PubMed: 33735165]
11. Darnell ME, Subbarao K, Feinstone SM, and Taylor DR. 2004. Inactivation of the coronavirus that induces severe acute respiratory syndrome, SARS-CoV. J. Virol. Methods 121: 85–91. [PubMed: 15350737]
12. Kumar M, Mazur S, Ork BL, Postnikova E, Hensley LE, Jahrling PB, Johnson R, and Holbrook MR. 2015. Inactivation and safety testing of Middle East respiratory syndrome coronavirus. J. Virol. Methods 223: 13–18. [PubMed: 26190637]
13. Case JB, Bailey AL, Kim AS, Chen RE, and Diamond MS. 2020. Growth, detection, quantification, and inactivation of SARS-CoV-2. Virology 548: 39–48. [PubMed: 32838945]
14. Inagaki H, Saito A, Sugiyama H, Okabayashi T, and Fujimoto S. 2020. Rapid inactivation of SARS-CoV-2 with deep-UV LED irradiation. Emerg. Microbes Infect 9: 1744–1747. [PubMed: 32673522]
15. Jureka AS, Silvas JA, and Basler CF. 2020. Propagation, inactivation, and safety testing of SARS-CoV-2. Viruses 12: 622.
16. Patterson EI, Prince T, Anderson ER, Casas-Sanchez A, Smith SL, Cansado-Utrilla C, Solomon T, Griffiths MJ, Acosta-Serrano Á, Turtle L, and Hughes GL. 2020. Methods of inactivation of SARS-CoV-2 for downstream biological assays. J. Infect. Dis 222: 1462–1467. [PubMed: 32798217]
17. Welch SR, Davies KA, Buczkowski H, Hettiarachchi N, Green N, Arnold U, Jones M, Hannah MJ, Evans R, Burton C, et al. 2020. Analysis of inactivation of SARS-CoV-2 by specimen transport media, nucleic acid extraction reagents, detergents, and fixatives. J. Clin. Microbiol 58: 58.

18. Widera M, Westhaus S, Rabenau HF, Hoehl S, Bojkova D, Cinatl J Jr., and Ciesek S. 2021. Evaluation of stability and inactivation methods of SARS-CoV-2 in context of laboratory settings. Med. Microbiol. Immunol. (Berl.) 210: 235–244. [PubMed: 34196781]

19. Darnell ME, and Taylor DR. 2006. Evaluation of inactivation methods for severe acute respiratory syndrome coronavirus in non-cellular blood products. Transfusion 46: 1770–1777. [PubMed: 17002634]

20. Rabenau HF, Cinatl J, Morgenstern B, Bauer G, Preiser W, and Doerr HW. 2005. Stability and inactivation of SARS coronavirus. Med. Microbiol. Immunol. (Berl.) 194: 1–6. [PubMed: 15118911]

21. Kariwa H, Fujii N, and Takashima I. 2006. Inactivation of SARS coronavirus by means of povidone-iodine, physical conditions and chemical reagents. Dermatology 212(Suppl 1): 119–123. [PubMed: 16490989]

22. Clemente A, Alba-Patiño A, Santopolo G, Rojo-Molinero E, Oliver A, Borges M, Aranda M, Del Castillo A, and de la Rica R. 2021. Immunodetection of lung IgG and IgM antibodies against SARS-CoV-2 via enzymatic liquefaction of respiratory samples from COVID-19 patients. Anal. Chem 93: 5259–5266. [PubMed: 33733739]

23. Haddad NS, Nguyen DC, Kuruvilla ME, Morrison-Porter A, Anam F,Cashman KS, Ramonell RP, Kyu S, Saini AS, Cabrera-Mora M, et al. 2021. One-stop serum assay identifies COVID-19 disease severity and vaccination responses. Immunohorizons 5: 322–335. [PubMed: 34001652]

24. Sterlin D, Mathian A, Miyara M, Mohr A, Anna F, Claër L, Quentric P, Fadlallah J, Devilliers H, Ghillani P, et al. 2021. IgA dominates the early neutralizing antibody response to SARS-CoV-2. Sci. Transl. Med 13: eabd2223.

25. Bernatchez JA, and McCall LI. 2020. Insights gained into respiratory infection pathogenesis using lung tissue metabolomics. PLoS Pathog 16: e1008662. [PubMed: 32663224]

26. Olszewski KL, Morrisey JM, Wilinski D, Burns JM, Vaidya AB,Rabinowitz JD, and Llin as M. 2009. Host-parasite interactions revealed by *Plasmodium falciparum metabolomics*. Cell Host Microbe 5: 191–199. [PubMed: 19218089]

27. Lourda M, Dzidic M, Hertwig L, Bergsten H, Palma Medina LM, Sinha I, Kvedaraite E, Chen P, Muvva JR, Gorin JB, et al. ; Karolinska KI/K COVID-19 Study Group. 2021. High-dimensional profiling reveals phenotypic heterogeneity and disease-specific alterations of granulocytes in COVID-19. Proc. Natl. Acad. Sci. USA 118: e2109123118. [PubMed: 34548411]

28. Mathew D, Giles JR, Baxter AE, Oldridge DA, Greenplate AR,Wu JE, Alanio C, Kuri-Cervantes L, Pampena MB, D'Andrea K, et al. ; UPenn COVID Processing Unit. 2020. Deep immune profiling of COVID-19 patients reveals distinct immunotypes with therapeutic implications. Science 369: eabc8511.

29. Stephenson E, Reynolds G, Botting RA, Calero-Nieto FJ, Morgan MD, Tuong ZK, Bach K, Sungnak W, Worlock KB, Yoshida M, et al. ; Cambridge Institute of Therapeutic Immunology and Infectious Disease-National Institute of Health Research (CITIID-NIHR) COVID-19 BioResource Collaboration. 2021. Single-cell multi-omics analysis of the immune response in COVID-19. Nat. Med 27: 904–916. [PubMed: 33879890]

30. Su Y, Chen D, Yuan D, Lausted C, Choi J, Dai CL, Voillet V,Duvvuri VR, Scherler K, Troisch P, et al. ; ISB-Swedish COVID19 Biobanking Unit. 2020. Multi-omics resolves a sharp disease-state shift between mild and moderate COVID-19. Cell 183: 1479–1495.e20. [PubMed: 33171100]

31. Zandi K, Musall K, Oo A, Cao D, Liang B, Hassandarvish P, Lan S, Slack RL, Kirby KA, Bassit L, et al. 2021. Baicalein and baicalin inhibit SARS-CoV-2 RNA-dependent-RNA polymerase. Micro-organisms 9: 893.

32. Kärber G 1931. Tabellen zur näaherungsweisen Bestimmung von Titern. Naunyn Schmiedebergs Arch. Exp. Pathol. Pharmakol 162: 480.

33. Reed LJ, and Muench H. 1938. A simple method of estimating fifty per cent endpoints. Am. J. Epidemiol 27: 493–497.

34. Ramakrishnan MA 2016. Determination of 50% endpoint titer using a simple formula. World J. Virol 5: 85–86. [PubMed: 27175354]

35. Stuyver LJ, Lostia S, Adams M, Mathew JS, Pai BS, Grier J,Tharnish PM, Choi Y, Chong Y, Choo H, et al. 2002. Antiviral activities and cellular toxicities of modified 2',3'-

dideoxy-2',3'-didehydrocytidine analogues. Antimicrob. Agents Chemother 46: 3854–3860. [PubMed: 12435688]

36. Chou T-C, and Talalay P. 1984. Quantitative analysis of dose-effect relationships: the combined effects of multiple drugs or enzyme inhibitors. Adv. Enzyme Regul 22: 27–55. [PubMed: 6382953]
37. Benjamini Y, Krieger AM, and Yekutieli D. 2006. Adaptive linear step-up procedures that control the false discovery rate. Biometrika 93: 491–507.
38. Dobin A, Davis CA, Schlesinger F, Drenkow J, Zaleski C, Jha S,Batut P, Chaisson M, and Gingeras TR. 2013. STAR: ultrafast universal RNA-seq aligner. Bioinformatics 29: 15–21. [PubMed: 23104886]
39. Stuart T, Butler A, Hoffman P, Hafemeister C, Papalexi E, Mauck WM 3rd, Hao Y, Stoeckius M, Smibert P, and Satija R. 2019. Comprehensive integration of single-cell data. Cell 177: 1888–1902.e21. [PubMed: 31178118]
40. Kim D, Lee JY, Yang JS, Kim JW, Kim VN, and Chang H. 2020. The architecture of SARS-CoV-2 transcriptome. Cell 181: 914–921.e10. [PubMed: 32330414]
41. Lu R, Zhao X, Li J, Niu P, Yang B, Wu H, Wang W, Song H, Huang B, Zhu N, et al. 2020. Genomic characterisation and epidemiology of 2019 novel coronavirus: implications for virus origins and receptor binding. Lancet 395: 565–574. [PubMed: 32007145]
42. Perkins SM, Webb DL, Torrance SA, El Saleeby C, Harrison LM, Aitken JA, Patel A, and DeVincenzo JP. 2005. Comparison of a real-time reverse transcriptase PCR assay and a culture technique for quantitative assessment of viral load in children naturally infected with respiratory syncytial virus. J. Clin. Microbiol 43: 2356–2362. [PubMed: 15872266]
43. Cook D, and Mandell L. 2000. Endotracheal aspiration in the diagnosis of ventilator-associated pneumonia. Chest 117(4, Suppl 2): 195S–197S. [PubMed: 10816036]
44. Scholte JB, van Dessel HA, Linssen CF, Bergmans DC, Savelkoul PH, Roekaerts PM, and van Mook WN. 2014. Endotracheal aspirate and bronchoalveolar lavage fluid analysis: interchangeable diagnostic modalities in suspected ventilator-associated pneumonia? J. Clin. Microbiol 52: 3597–3604. [PubMed: 25078907]
45. Kurth J, Waldmann R, Heith J, Mausbach K, and Burian R. 1999. Efficient inactivation of viruses and mycoplasma in animal sera using UVC irradiation. Dev. Biol. Stand 99: 111–118. [PubMed: 10404882]
46. Terpstra FG, van 't Wout AB, Schuitemaker H, van Engelenburg FA,Dekkers DW, Verhaar R, de Korte D, and Verhoeven AJ. 2008. Potential and limitation of UVC irradiation for the inactivation of pathogens in platelet concentrates. Transfusion 48: 304–313. [PubMed: 18028277]
47. Simón-Manso Y, Lowenthal MS, Kilpatrick LE, Sampson ML,Telu KH, Rudnick PA, Mallard WG, Bearden DW, Schock TB, Tchekhovskoi DV, et al. 2013. Metabolite profiling of a NIST Standard Reference Material for human plasma (SRM 1950): GC-MS, LC-MS, NMR, and clinical laboratory analyses, libraries, and web-based resources. Anal. Chem 85: 11725–11731. [PubMed: 24147600]
48. de Jager TL, Cockrell AE, and Du Plessis SS. 2017. Ultraviolet light induced generation of reactive oxygen species. Adv. Exp. Med. Biol 996: 15–23. [PubMed: 29124687]
49. Gruber J, Tang SY, Jenner AM, Mudway I, Blomberg A, Behndig A, Kasiman K, Lee CY, Seet RC, Zhang W, et al. 2009. Allantoin in human plasma, serum, and nasal-lining fluids as a bio-marker of oxidative stress: avoiding artifacts and establishing real in vivo concentrations. Antioxid. Redox Signal 11: 1767–1776. [PubMed: 19388825]
50. Lee BC, and Gladyshev VN. 2011. The biological significance of methionine sulfoxide stereochemistry. Free Radic. Biol. Med 50: 221–227. [PubMed: 21075204]
51. Maghzal GJ, Leck MC, Collinson E, Li C, and Stocker R. 2009. Limited role for the bilirubin-biliverdin redox amplification cycle in the cellular antioxidant protection by biliverdin reductase. J. Biol. Chem 284: 29251–29259. [PubMed: 19690164]
52. Chattopadhyay PK, and Roederer M. 2012. Cytometry: today's technology and tomorrow's horizons. Methods 57: 251–258. [PubMed: 22391486]

53. Brummelman J, Haftmann C, Núñez NG, Alvisi G, Mazza EMC, Becher B, and Lugli E. 2019. Development, application and computational analysis of high-dimensional fluorescent antibody panels for single-cell flow cytometry. Nat. Protoc 14: 1946–1969. [PubMed: 31160786]

54. Perfetto SP, Chattopadhyay PK, and Roederer M. 2004. Seventeen-colour flow cytometry: unravelling the immune system. Nat. Rev. Immunol 4: 648–655. [PubMed: 15286731]

55. Roederer M, De Rosa S, Gerstein R, Anderson M, Bigos M, Stovel R, Nozaki T, Parks D, Herzenberg L, and Herzenberg L. 1997. 8 color, 10-parameter flow cytometry to elucidate complex leukocyte heterogeneity. Cytometry 29: 328–339. [PubMed: 9415416]

56. Woodruff MC, Ramonell RP, Nguyen DC, Cashman KS, Saini AS, Haddad NS, Ley AM, Kyu S, Howell JC, Ozturk T, et al. 2020. Extrafollicular B cell responses correlate with neutralizing antibodies and morbidity in COVID-19. Nat. Immunol 21: 1506–1516. [PubMed: 33028979]

57. Silvin A, Chapuis N, Dunsmore G, Goubet AG, Dubuisson A, Derosa L, Almire C, H enon C, Kosmider O, Droin N, et al. 2020. Elevated calprotectin and abnormal myeloid cell subsets discriminate severe from mild COVID-19. Cell 182: 1401–1418.e18. [PubMed: 32810439]

58. Wang J, Mauser A, Chao SF, Remington K, Treckmann R, Kaiser K, Pifat D, and Hotta J. 2004. Virus inactivation and protein recovery in a novel ultraviolet-C reactor. Vox Sang 86: 230–238. [PubMed: 15144527]

59. Cutts TA, Cook BWM, Poliquin PG, Strong JE, and Theriault SS. 2016. Inactivating Zaire ebolavirus in whole-blood thin smears used for malaria diagnosis. [Published erratum appears in 2021 *J. Clin. Microbiol*. 59: e00643–21.] J. Clin. Microbiol 54: 1157–1159. [PubMed: 26865684]

60. Mok CK, Goh VSL, Ma L, and Chu JJH. 2020. Establish a standard inactivation protocol for virus research in a high containment laboratory. Int. J. Infect. Dis 101(Suppl 1): 254.

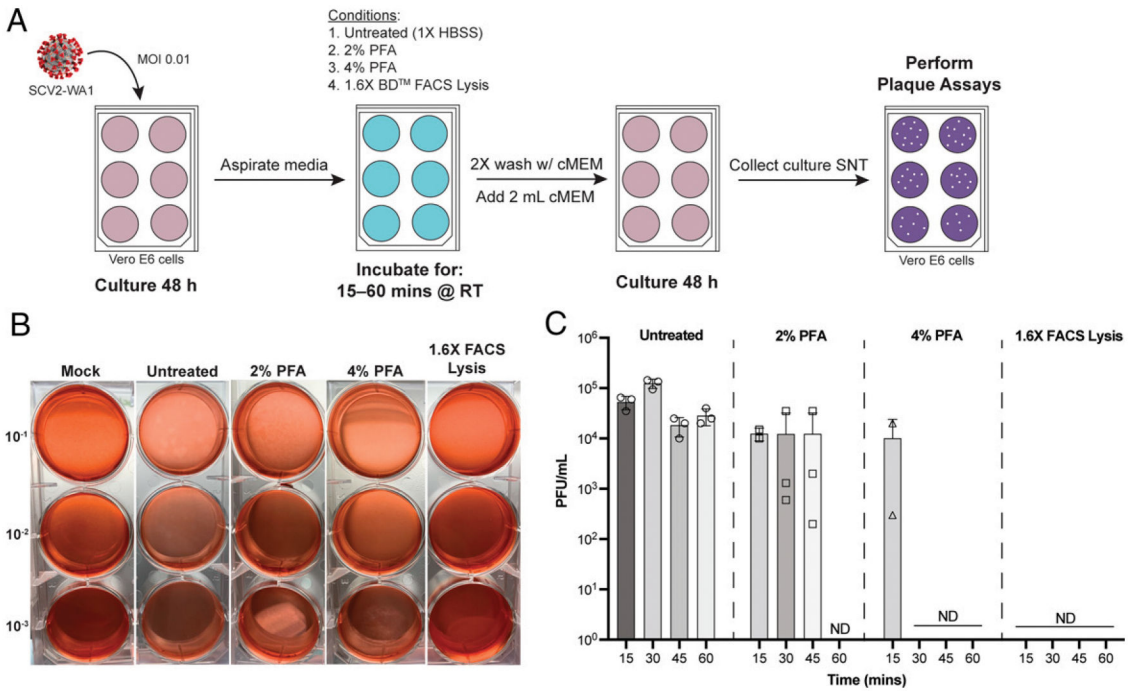

FIGURE 1. Fixation with commercially available fixatives promote complete inactivation of SARS-CoV-2–infected cells amenable to flow cyto-metric analyses

(**A**) Schematic of inactivation time course performed to evaluate inactivation efficiency. SNT, supernatant. (**B**) Representative plaque assays from inactivation time course. (**C**) Quantification of viral load for the four fixatives across the four time points evaluated. Data are averaged of duplicates from two independent experiments. ND, not detected (by plaque assay).

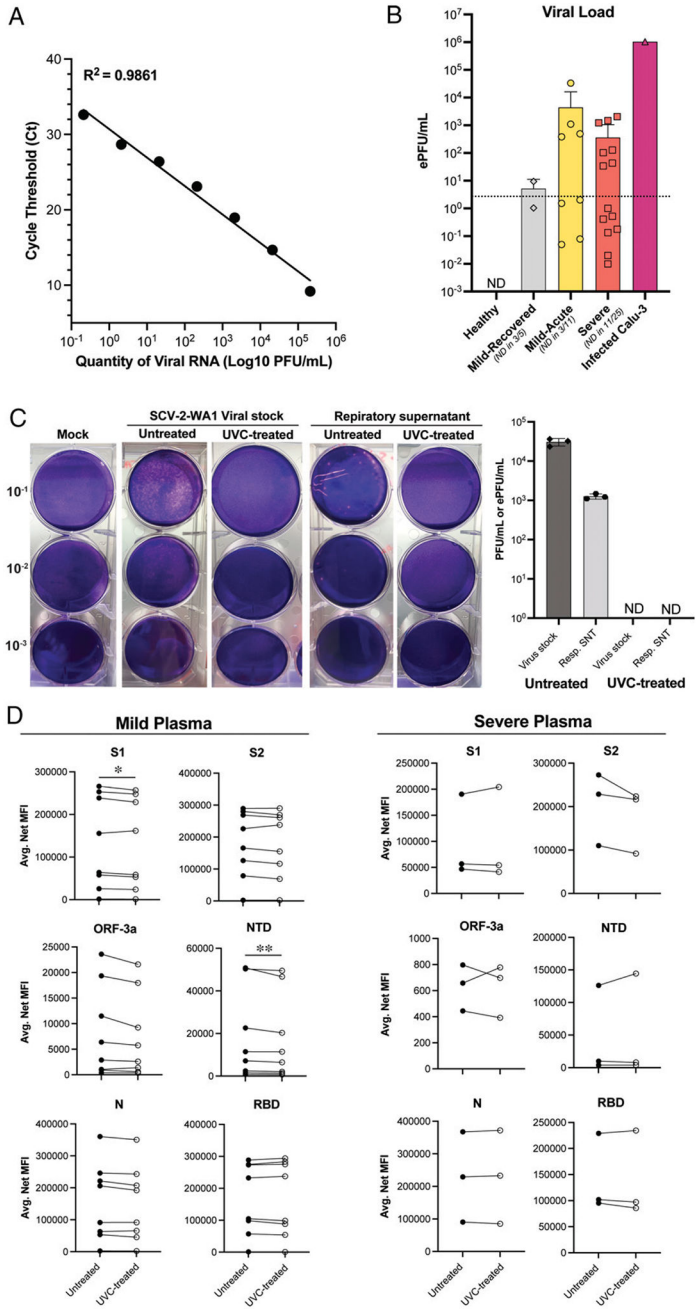

FIGURE 2. UVC irradiation exposure for 30 min inactivates SARS-CoV-2 with minimal effects on protein/Ab detection assays

(**A**) Viral curve generated from serially dilutedSCV2-WA1 stock of a known titer to extrapolate ePFU/ml from RT-qPCR data. Data are averages of duplicates from a single experiment. (**B**) Viral load (ePFU/ml) in respiratory supernatant (Resp.SNT) from non-induced sputum (healthy and mild) and endotracheal aspirate (ETA; severe) samples using the viral curve generated in (A).Dotted line indicates lower limit of quantification for the ePFU conversion determined by the lowest dilution of stock virus (10^{-6}) detected by RT-qPCR. ND, not detected (by RT-qPCR). Data are averages of duplicates from a single

experiment. (**C**) Representative plaque assays from stockSCV2-WA1 virus and respiratory supernatant (Resp. SNT) samples and quantification of viral load (PFU/ml for SCV2-WA1 stock and ePFU/ml for Resp. SNT from B) before and after UVC treatment (30 min at ~4000 μW/cm^2). Data are averages of duplicates from two independent experiments. ND, not detected (by plaque assay). (**D**) Comparison of SARS-CoV-2 Ab measurements in untreated and UVC-treated plasma samples from mild and severe COVID-19 patients.Data are averaged duplicates from two independent experiments. Statistical significance was determined using two-tailed paired ratio *t* tests orWilcoxon matched-pairs signed rank tests (*see* Materials and Methods). All comparisons were not significant unless indicated otherwise. *$p = 0.0237$, **$p = 0.0078$.

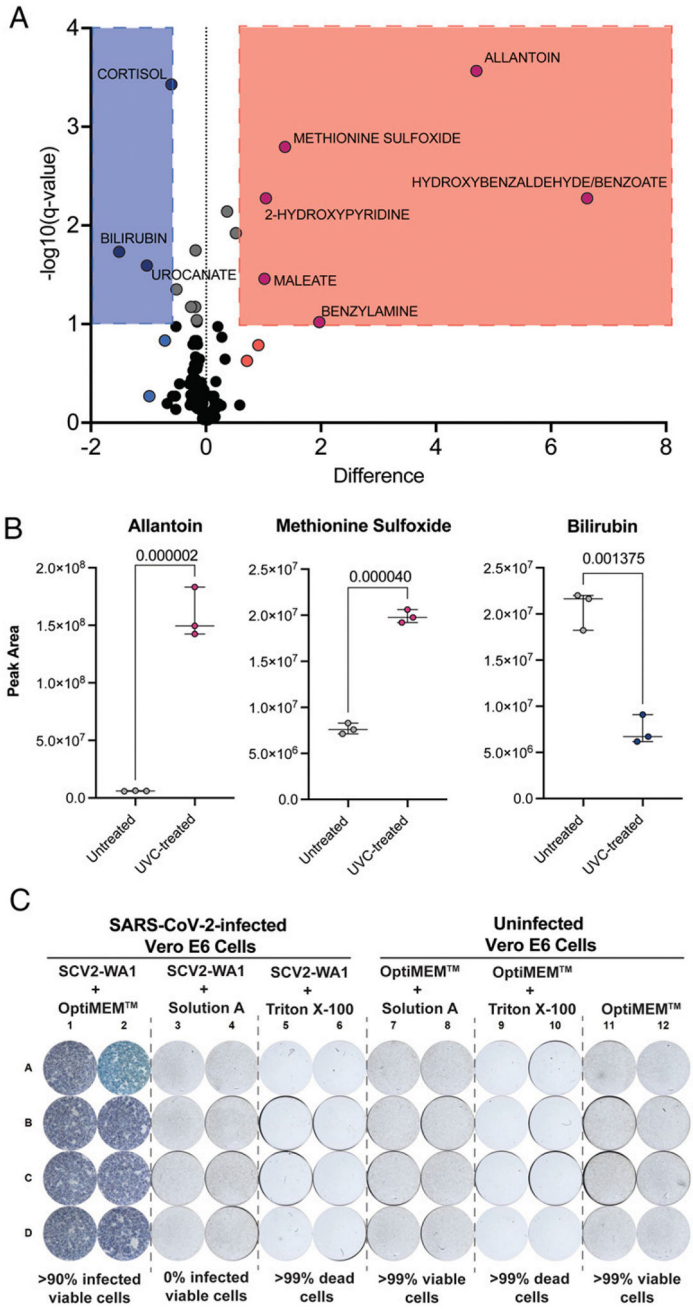

FIGURE 3. Metabolite extraction solvent (solution A) completely inactivates SARS-CoV-2 and maintains sample quality for downstream metabolomics assays

(**A**) Volcano plot (FDR <10%) displaying differentially expressed metabolites in untreated versus UVC-treated NIST (standard) plasma samples. (**B**) Example plots of three representatives differentially expressed, redox-active metabolites in untreated versus UVC-treated NIST plasma samples. Analyzed by unpaired *t* tests for untreated versus UVC-treated replicates, using the adaptive linear step-up method to control the FDR (*see* Materials and Methods). Data are averaged duplicates from a single experiment. (**C**) FRNA results

evaluating inactivation of the metabolite extraction solvent (solution A) in the standard metabolomic sample processing procedure (*see* Materials and Methods) and Triton X-100.

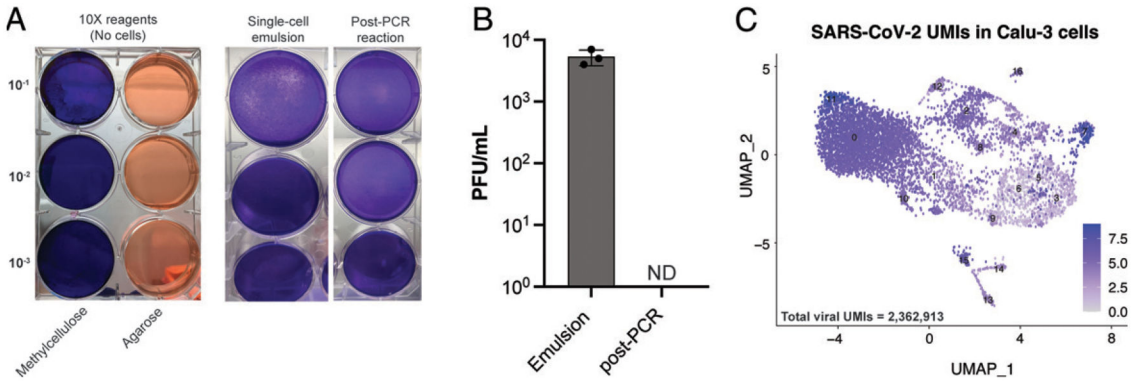

FIGURE 4. Heat inactivation during cDNA synthesis completely inactivates SARS-CoV-2 in scRNA-seq emulsions

(**A**) Representative plaque assays performed using 10x Genomics emulsion reagents alone (without cells) to evaluate reagent cytotoxicity on Vero E6 cells and single-cell emulsion with SCV2-WA1–infected Vero E6 cells (MOI of 0.04), and the same emulsion after cDNA synthesis PCR reaction (45 min at 53°C followed by 5 min at 85°C). Duplicate samples were evaluated in two independent experiments. (**B**) Quantification of viral load in single-cell emulsions of SCV2-WA1–infected Calu-3 cells (MOI of 0.04) immediately after encapsulation and following PCR reaction for cDNA synthesis. $n = 3$ independent samples reported as averaged duplicates from a single experiment. ND, not detected (by plaque assay). (**C**) Uniform manifold approximation and projection (UMAP) visualization of scRNA-seq data from SCV2-WA1–infected Calu-3 cells (MOI of 0.04; $n = 8061$ cells) showing expression of the 12 SARS-CoV-2 genes and total viral UMIs (inset).